Stoichiometry and adhesion of Nb/Al_2O_3

W. Zhang
Princeton Materials Institute, Princeton University, Princeton, New Jersey 08540

J. R. Smith
Delphi Research Labs, Warren, Michigan 48090

(Received 14 February 2000)

We examine the relative stability of both stoichiometric and nonstoichiometric Nb/Al_2O_3 interfaces and Al_2O_3 surfaces. Results of first-principles computations of surface and interfacial atomic relaxations, electron-density distributions, and total energies are presented. We found that while the Al-terminated $Al_2O_3(0001)$ surface is stable relative to the O-terminated surface, interface formation with Nb can reverse the stability, depending on the oxygen partial pressure. This interfacial structure is consistent with recent experimental results. Finally, we computed some of the energetics associated with the diffusion of Al into Nb across the Nb/Al_2O_3 interface. Our results are consistent with Al migration into the Nb at temperatures of the order of 10^3 K, as reported experimentally.

I. INTRODUCTION

Adhesion at metal/ceramic interfaces is not only an intriguing materials research subject, but it is also of considerable practical importance. Electronic packaging, corrosion-resistant coatings, and high-temperature composite materials depend on adhesion between metals and ceramics. In turn, this adhesion is dependent on the atomic structure of the interface.[1–9] The $Nb(111)/\alpha\text{-}Al_2O_3(0001)$ interface is a good test bed for understanding metal/ceramic adhesion because[1–9] the interface is almost strain-free, the adhesive bond is relatively strong, the coefficients of thermal expansion of the two materials are nearly the same, the interface is atomically abrupt, and the interfacial atomic structure is well characterized.

Bruley *et al.*[5] have prepared the $Nb(111)/\alpha\text{-}Al_2O_3(0001)$ interface via molecular beam epitaxy, and they found that the niobium atoms are bonded to an oxygen-terminated Al_2O_3 surface. This interface is not stoichiometric, i.e., the ratio of oxygen atoms to aluminum atoms is not 3 to 2, but rather the interface is oxygen-rich. This is particularly interesting because, as we will see in the following and consistent with earlier work,[10] even at high oxygen pressures the free (clean) $Al_2O_3(0001)$ surface is Al-terminated, with the oxygen-terminated surface being significantly higher in energy than the Al-terminated surface. In the following we will examine from first principles the effect of the Nb/Al_2O_3 interaction on the Al_2O_3 termination. We will see that the Nb/Al_2O_3 interaction can in fact reverse the relative stability of oxygen and Al-terminated Al_2O_3 interfaces as the oxygen chemical potential and oxygen partial pressure increases, consistent with Ref. 5. An oxygen-pressure dependence of metal/alumina bonding is also consistent with a reported[11] dependence of metal/alumina works of adhesion on oxygen partial pressure. To our knowledge, this is the first time the stable interfacial structure has been predicted for a metal/ceramic oxide interface.

Finally, we compute energetics relative to a potential Al diffusion from the alumina into the niobium across the Nb/Al_2O_3 interface. We will see that our results are consistent with experimental observations of Al diffusion into the Nb at temperatures of order 10^3 K.

II. COMPUTATIONAL METHODS

The Nb/Al_2O_3 interface has been modeled by Batirev, Alavi, and Finnis[7] within a pseudopotential approximation. Here we go beyond that approximation, including all core electrons in our computations. Our electronic structure calculations were performed using an accurate full-potential linearized augmented plane-wave (FLAPW) method[12] including local orbital extensions[13] to increase flexibility of the basis set. The structures are fully relaxed by the Hellmann-Feynman forces.[14] The muffin-tin radii for Nb, Al, and O atoms turned out to be 1.1, 0.85, and 0.74, respectively, where length units throughout the paper are ångstroms. We included plane waves with an energy cut off of 18.4 Ry to ensure force convergence. Five special k points in the irreducible part of the first surface Brillouin zone are used to generate the electron-density distributions. Atomic locations are assumed to be converged when the force on each atom is less than 0.03 eV/Å. Results using both the local-density approximation[15] (LDA) and the presumably more accurate generalized-gradient approximation (GGA) of Perdew, Burke, and Ernzerhof[16] are all presented in order to determine the importance of the GGA in this application.

We used a supercell approach to simulate the interface. Two Nb(111) slabs are adhered to both sides of an Al_2O_3 slab, maintaining inversion symmetry relative to the center of the Al_2O_3 slab. These slabs repeat periodically to infinity parallel to the interface, but are of finite dimension perpendicular to the interface. Each Nb slab is six atomic layers thick and the Al_2O_3 slab typically contains four oxygen atomic layers and eight aluminum atomic layers. Each cell then contains two $Nb(111)/Al_2O_3(0001)$ interfaces, and we maintain 8 Å of vacuum between the outer Nb surfaces in adjacent supercells. Thicker $Al_2O_3(0001)$ slabs have been treated,[17] and we will see that our results agree well with

TABLE I. Relaxation results for the surface systems Nb monolayer on O-terminated alumina $[(Nb)_1(Al_2O_3)_O]$, Al-terminated $[(Al_2O_3)_{Al}]$, and O-terminated $[(Al_2O_3)_O]$. All interplanar spacings are given as a percentage increase (plus) or decrease (minus) relative to the Al_2O_3 bulk spacings.

	$(Nb)_1(Al_2O_3)_O$		$(Al_2O_3)_{Al}$		$(Al_2O_3)_O$	
	LDA	GGA	LDA	GGA	LDA	GGA
Nb(Al)-O	−24.23	−22.31	−85.84	−86.02		
O-Al	11.99	17.03	1.10	3.58	−23.13	−20.09
Al-Al	−38.73	−41.23	−42.86	−38.74	2.59	3.00
Al-O	10.72	14.03	17.48	19.06	9.99	13.57
O-Al	−2.02	1.10	1.00	2.70	−3.33	0.40

those of others where available. We define these interfaces for which the $Al_2O_3(0001)$ is Al-terminated as $Nb/(Al_2O_3)_{Al}$. The oxygen-terminated interface, $Nb/(Al_2O_3)_O$, is defined in the same way, except that the outer Al layer at the interface is removed, with the atoms of the outer Nb layer falling at the Al sites. This is consistent with the experimental results.[5] No symmetry besides inversion is required. Only the two Al layers in the center of the supercell are fixed, with all other atoms allowed to relax freely in the three dimensions. The experimental lattice constants of the Al_2O_3 crystal[18] $(a/c = 4.7628/13.0032)$, were used for these two Al layers, so the Nb(111) must stretch by 1.72% (see next section) to be commensurate. We expect the effects of misfit dislocations to be small.[19]

III. RESULTS

A. Bulk Nb

Our calculated bulk lattice constants for Nb are 3.23 in LDA and 3.31 in the (more accurate) GGA, in good agreement with the measured value[20] of 3.30. The LDA interfacial lattice mismatch between the two materials is 2.86%, while the GGA value is 1.72% as noted above. For the unstrained Nb(111) surface, the calculated surface energies are 2.95 J/m^2 (LDA) and 2.43 J/m^2 (GGA), being close to the polycrystalline experimental value of 2.44 J/m^2.[21]

B. Atomic relaxations of the Al_2O_3 surface and Nb/Al_2O_3 interfaces

1. Al_2O_3 free surface and Al_2O_3 with adsorbed Nb monolayer

We first computed the relaxation of the (1×1) Al-terminated, $(Al_2O_3)_{Al}$, and oxygen-terminated, $(Al_2O_3)_O$, alumina surface. Next we determined the relaxation of a Nb monolayer on O-terminated alumina, $(Nb)_1(Al_2O_3)_O$, with the Nb atoms located at those sites occupied by Al atoms on $(Al_2O_3)_{Al}$. These systems were chosen in order to compare with earlier work done on some of them and because they are the substrates on which we will deposit Nb. The results for the atomic surface relaxations are shown in Table I. There and in Table II we list planar relaxations of the atomic layers, even though we have allowed for full three-dimensional relaxation of each atom. We found that the atoms remained coplanar to within 0.02 Å. The relaxations for $(Al_2O_3)_{Al}$ are similar to the results of earlier computations.[7,10,17,22] The most striking aspect here is the quite large relaxation of the outer Al layer, with it becoming almost coplanar with the outer O layer. The relaxation of the spacing between outer O layer of $(Al_2O_3)_O$ and the Al layer beneath it is an order of magnitude larger than the corresponding value for $(Al_2O_3)_{Al}$, but it is substantially less than the spacing decrease between the outer Al layer of $(Al_2O_3)_{Al}$ and the O layer beneath it. We know of no earlier theoretical results for relaxations of $(Al_2O_3)_O$ with which we can compare the various interplanar results of Table I. We found that the Nb monolayer on O-terminated Al_2O_3 has an inward relaxation[23] that is significantly less than the outer Al layer of $(Al_2O_3)_{Al}$. This is presumably due to the larger size of the Nb atoms (ions) relative to the Al atoms (ions). The threefold-bonded O atoms nearest to the Nb atoms are also squeezed outward (essentially within plane, with the distance between those O atoms increasing by as much as 0.28 Å = 6% of the in-plane lattice constant) and rotated through an angle of 6°. This also squeezes the Al layer below the outer O layer, leading to a relatively large increase in O-Al interplanar spacing. For $(Al_2O_3)_{Al}$, although the top O layer is almost coplanar with the top Al layer, because of the relatively small size of the of Al^{3+} ions, the O atoms are squeezed outward by a smaller distance, and the O rotation is much less (<2°). In Ref. 6 an outward relaxation of the Nb monolayer was reported. We do not know at this time why our results are different.

It is interesting to look at electron-density contours shown in Fig. 1. These are the self-consistent density distributions minus the overlapping atomic densities. The electron transfer to the O atoms is apparent for both $(Al_2O_3)_{Al}$ and $(Nb)_1(Al_2O_3)_O$. There is in addition a polarization of the Nb site of $(Nb)_1(Al_2O_3)_O$. A comparison of the outer Al in Fig. 1(a) and the Nb of Fig. 1(b) is also suggestive of the Al and Nb size and location differences.

2. Niobium/alumina interfaces

Results for the relaxation of atomic positions at the $Nb/(Al_2O_3)_{Al}$ and $Nb/(Al_2O_3)_O$ interfaces are found in Table II. Now we have, as mentioned earlier, six atomic layers of Nb on either side of the alumina slab. Reasonable agreement is obtained with the results of Ref. 7. The relaxation of these interfaces shows characteristics similar to those of Fig. 1 and Table I. For $Nb/(Al_2O_3)_{Al}$, the outer O in-plane radial strain (<1% of the in-plane lattice constant) and rotation (<2°) are almost negligible. But, with Nb replacing Al as in $Nb/(Al_2O_3)_O$, the outer O in-plane radial strain and rotation increase to 3% of the in-plane lattice constant and 4°, respectively. Perhaps the most interesting effect of the thicker Nb layers is found in the much smaller decrease in distance be-

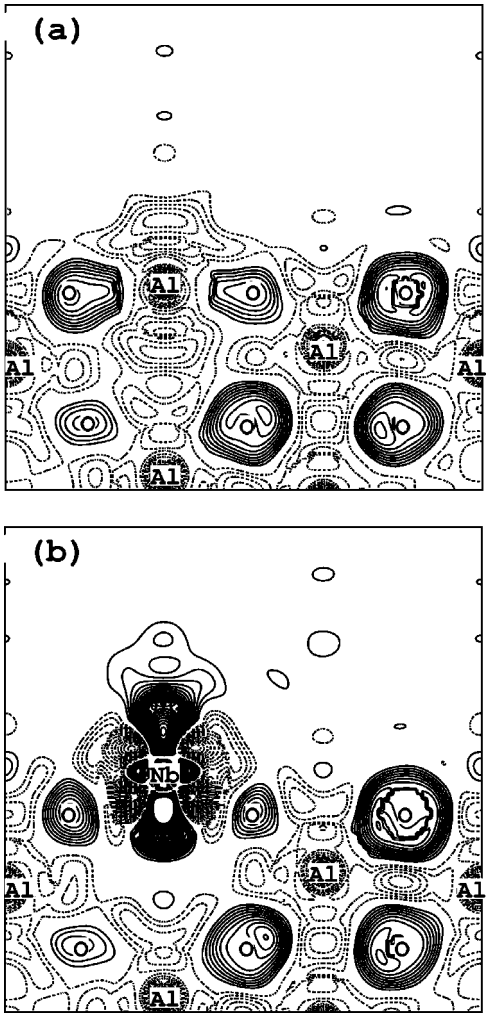

FIG. 1. Contour plots of valence-electron-density differences for (a) the $(Al_2O_3)_{Al}$ and (b) the $(Nb)_1(Al_2O_3)_O$ surfaces. This is obtained by subtracting the superposition of valence electron densities of neutral atoms from the self-consistent density distributions. The solid lines indicate electron accumulation, and the dashed lines depletion.

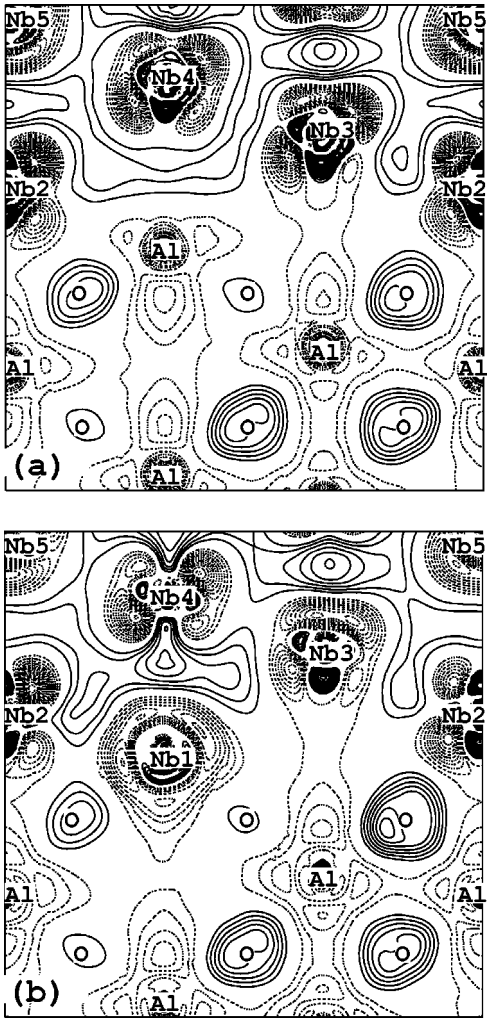

FIG. 2. Electron-density difference contours for (a) $Nb/(Al_2O_3)_{Al}$ and (b) $Nb/(Al_2O_3)_O$. These are the self-consistent density distributions minus the superposition of valence-electron densities of neutral atoms. The solid lines indicate electron accumulation, while the dashed lines indicate depletion.

tween the outer Al and outer O layers of $Nb/(Al_2O_3)_{Al}$ [7.5% for $Nb/(Al_2O_3)_{Al}$ and 86.0% for $(Al_2O_3)_{Al}$], and the significantly larger distance between the outer O layer and the first Nb layer [0.637 Å for $(Nb)_1(Al_2O_3)_O$ and 1.125 Å for $Nb/(Al_2O_3)_O$].

This is also apparent in the electron-density contour plots for $Nb/(Al_2O_3)_{Al}$ shown in Fig. 2(a) and for $Nb/(Al_2O_3)_O$ shown in Fig. 2(b), in comparison with Figs. 1(a) and 1(b), respectively. This is perhaps consistent with the results reported in Ref. 25 for $\frac{1}{3}$ monolayer to monolayer coverages of Nb on τ-Al_2O_3, indicating that the Nb desorption energies decrease with coverage. The strong Nb polarization evident in Fig. 1(b) does not appear in Figs. 2(a) and 2(b), the ''dangling'' Nb bond seemingly replaced by bonding within the Nb. There appears to be a fundamental difference between the Nb atomic layers nearest the alumina [Nb2 in Fig. 2(a)] and Nb1 in Fig. 2(b)]. For $Nb/(Al_2O_3)_{Al}$, Nb2 looks similar to Nb3 and Nb4 [see Fig. 2(a)]. However, for $Nb/(Al_2O_3)_O$ shown in Fig. 2(b), there is a marked difference between the Nb layer nearest the alumina, Nb1, Nb2, and Nb3 of Fig. 2(b). That is, Nb1 looks more ionic and less metallic than Nb2 and Nb3. This is to be expected because Nb1 is replacing the Al layer.

Finally, Table III contains the works of separation for $Nb/(Al_2O_3)_{Al}$ and $Nb/(Al_2O_3)_O$. These are the energy per cross-sectional area at large interfacial separation minus the corresponding value at equilibrium separation for Nb and $(Al_2O_3)_{Al}$ or $(Al_2O_3)_O$.

Perhaps the most striking result from Table III is the rather large difference between the $Nb/(Al_2O_3)_{Al}$ and the $Nb/(Al_2O_3)_O$ works of separation. The bond energies of the $Nb/(Al_2O_3)_O$ interface are over 3 times those of the $Nb/(Al_2O_3)_{Al}$ interface. This is perhaps consistent with the ionic nature of the bonds in the $Nb/(Al_2O_3)_O$ interface as compared to the more metallic nature of the bonds in the $Nb/(Al_2O_3)_{Al}$ interface, as we saw in Figs. 2(a) and 2(b). We will see in the next section that the $(Al_2O_3)_O$ surface energy tends to be substantially larger than the $(Al_2O_3)_{Al}$ surface energy, even for relatively large oxygen partial pressures. Since these are the corresponding Al_2O_3 surfaces for the two different terminations when the Nb/Al_2O_3 interfaces are at

TABLE II. Results for relaxations in atomic positions of the Nb/$(Al_2O_3)_O$ and Nb/$(Al_2O_3)_{Al}$ interfaces. Interplanar spacings are given as a percentage increase (plus) or decrease (minus) relative to the corresponding bulk spacing (Refs. 18 and 24). While the computation includes six Nb layers, we give results for the four Nb layers closest to the Al_2O_3 surface.

	Nb/$(Al_2O_3)_O$			Nb/$(Al_2O_3)_{Al}$		
	LDA	GGA	Ref. 7	LDA	GGA	Ref. 7
Nb4-Nb3	−5.7	−6.49	−2.4	−7.6	−4.6	−3.1
Nb3-Nb2	9.5	12.9	12.2	−4.7	−9.0	3.6
Nb2-Nb1(Al)	−37.2	−35.4	−26.3	5.5	5.3	−2.1
Nb1(Al)-O	33.8	37.9	30.4	−10.8	−7.5	−2.2
O-Al	2.41	8.05	10.1	1.21	4.67	8.5
Al-Al	−16.7	−19.6	−17.2	−17.0	−17.5	−12.9
Al-O	2.8	7.7	7.1	3.7	7.3	8.7
O-Al	−2.0	2.4	−0.9	−2.6	1.3	1.7

large separation, these surface energy results are not inconsistent with the results of Table III. The works of separation seem relevant to fracture, particularly at relatively rapid crack velocities. That is, suppose, e.g., that the oxygen partial pressure is such that the interface is oxygen terminated (see Sec. II C). Then, if the fracture were rapid enough, perhaps the interfacial bonds would be broken before the $(Al_2O_3)_O$ would have a chance to relax to the (lower-energy) $(Al_2O_3)_{Al}$ surface. In that case, the Nb/$(Al_2O_3)_O$ work of separation would be the relevant quantity of interest.

C. Bonding energies and deviations from stoichiometry

We can get further insight into the differences noted previously between the adhesive interactions found in Nb/$(Al_2O_3)_O$ and Nb/$(Al_2O_3)_{Al}$ by considering surface and adhesive energies. This will lead us to formulate the effect of deviations from stoichiometry on adhesion. First, our $(Al_2O_3)_{Al}$ surface energy is 2.59 J/m^2 in LDA. This is a little higher than the LDA result of 1.98 J/m^2 reported by Felice and Northrup.[10(a)] Our GGA result of 2.15 J/m^2 is rather close to the GGA results of 2.13 J/m^2 (Wang *et al.*)[10(b)] and 1.95 J/m^2.[7]

It is not straightforward to report the surface energy of $(Al_2O_3)_O$ because that surface is not stoichiometric. This is also true for the Nb/$(Al_2O_3)_O$ interface. In these cases, we must take into account the fact that[11] the oxygen partial pressure and, correspondingly, the oxygen chemical potential can vary. To proceed, we compute the Gibbs free energy[10,26] to analyze interfacial stability. The Gibbs free energy G of the slab at pressure P and temperature T is

$$G = E_{\rm tot} - N_{\rm O}\mu_{\rm O} - N_{\rm Al}\mu_{\rm Al} - N_{\rm Nb}\mu^B_{\rm Nb} + PV - TS. \quad (1)$$

Here $E_{\rm tot}$ is the total energy of the slab, $\mu_{\rm O}$, $\mu_{\rm Al}$, and $\mu^B_{\rm Nb}$ are the chemical potentials of oxygen, aluminum, and niobium respectively, and $N_{\rm O}$, $N_{\rm Al}$, and $N_{\rm Nb}$ are the numbers of the corresponding atoms in the cell, with $N_{\rm O}\mu_{\rm O} + N_{\rm Al}\mu_{\rm Al} + N_{\rm Nb}\mu^B_{\rm Nb}$ being the corresponding bulk energies of alumina and niobium, respectively. By subtracting the bulk energies, G contains only surface and interfacial energies.

TABLE III. Works of separation in J/m^2.

	LDA	GGA	Ref. 7
Nb/$(Al_2O_3)_{Al}$	3.3	2.6	2.8
Nb/$(Al_2O_3)_O$	12.3	10.6	9.8

Equation (1) can be simplified. First, for typical pressures and temperatures, the terms PV and TS can be neglected. Second, note $\mu_{Al_2O_3} \equiv 3\mu_O + 2\mu_{Al}$, where $\mu_{Al_2O_3}$ is the chemical potential of bulk alumina. Equation (1) becomes

$$G = E_{\rm tot} - \frac{N_{\rm Al}}{2}\mu_{Al_2O_3} - (N_{\rm O} - \tfrac{3}{2}N_{\rm Al})\mu_{\rm O} - N_{\rm Nb}\mu^B_{\rm Nb}. \quad (2)$$

For the stoichiometric interface, the coefficient of the term containing $\mu_{\rm O}$ vanishes. Since $\mu_{Al_2O_3}$ and $\mu_{\rm Nb}$ are bulk quantities, G is uniquely defined in this case, independent of $\mu_{\rm O}$. For nonstoichiometric interfaces, G will be a function of $\mu_{\rm O}$, or, equivalently, of $\Delta\mu_{\rm O} \equiv \mu_{\rm O} - \mu^{\rm gas}_{\rm O}$.

To apply Eq. (2) to free (clean) Al_2O_3(0001) surfaces, we set $N_{\rm Nb} = 0$. The range of interest for $\Delta\mu_{\rm O}$ is

$$-\tfrac{1}{3}\Delta H_{Al_2O_3} \leqslant \Delta\mu_{\rm O} \leqslant 0, \quad (3)$$

and where $\Delta H_{Al_2O_3}$ is the heat of formation of alumina, which we take[27] to be 17.37 eV. The inequalities of Eq. (3) arise from our expectation that the nonstoichiometric material lies somewhere in between metallic Al and (molecular) oxygen.

The results are shown in the inset of Fig. 3 (see also Ref. 10). The input of the empirical value for $\Delta H_{Al_2O_3}$ implies that $\mu^{\rm gas}_{\rm O}$ is the oxygen gas chemical potential in its standard state, i.e., at 1 atm of pressure and $T = 298.15$ K. This locates the origin of the abscissa in Fig. 3. It should be remembered, however, that our total-energy computations are carried out at $T = 0$ K, as is typical of state-of-the-art first-principles methods. This is an approximation relative to comparison with experimental results at $T > 0$ K, but it has been a successful approximation for researchers comparing total-energy differences in solids. The vertical lines in the inset show the limits indicated by Eq. (3). In Fig. 3 we see, as expected, that $(Al_2O_3)_{Al}$ is independent of $\Delta\mu_{\rm O}$ since it is stoichiometric. Also, $(Al_2O_3)_O$ depends linearly on $\Delta\mu_{\rm O}$, consistent with Eq. (2). The GGA surface energies are a little

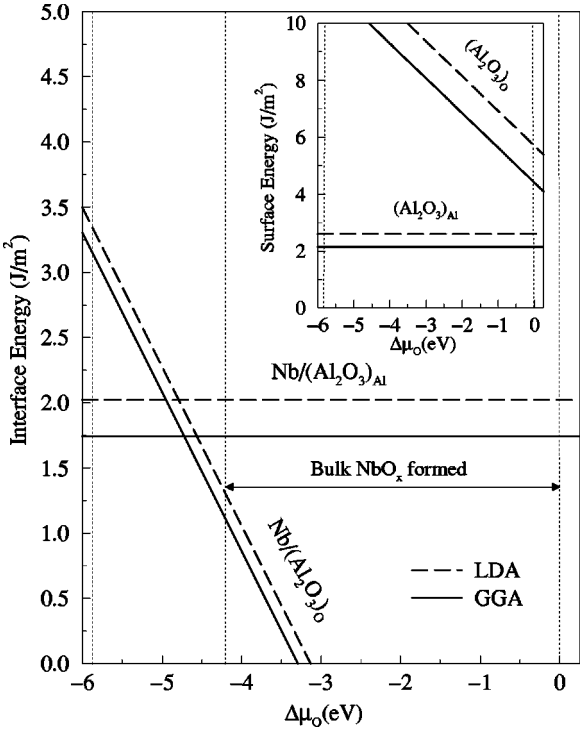

FIG. 3. Interfacial energies of the $Nb/(Al_2O_3)_{Al}$ and $Nb/(Al_2O_3)_O$ interfaces vs $\Delta\mu_O \equiv \mu_O - \mu_O^{gas}$, i.e., vs the difference between the oxygen chemical potential in the material and its value for the gas. The inset shows the surface energy vs $\Delta\mu_O$ for the free (clean) alumina surfaces, $(Al_2O_3)_{Al}$ and $(Al_2O_3)_O$. The solid lines are for GGA, and the dashed lines are for LDA calculations (see Sec. II).

lower than the LDA values, but the relative energies and trends are quite similar. Most interesting is the fact that, as mentioned above and consistent with earlier work,[10] the $(Al_2O_3)_{Al}$ surface is stable (lower surface energy) over the entire range of oxygen pressures [Eq. (3)].

Next, let us apply Eq. (2) to the Nb/Al_2O_3 interface. In this case, we take E_{tot} to be the total energy of the slab minus the energy of the two Nb(111) surfaces, so that G becomes a purely interfacial energy γ_I. As a check, we also determined the interfacial energy by combining the computed works of separation γ_S (Table III) and the computed surface energies σ_{Nb} and $\sigma_{Al_2O_3}$ ($\gamma_I = \sigma_{Nb} + \sigma_{Al_2O_3} - \gamma_S$). Excellent agreement was found.

Results are shown in Fig. 3. The vertical lines at $\Delta\mu_O = 0$ and near $\Delta\mu_O = -6$ designate the range shown in Eq. (3). Again, the stoichiometric interface, $Nb/(Al_2O_3)_{Al}$, has an interfacial energy that is independent of $\Delta\mu_O$, as expected. Also, $Nb/(Al_2O_3)_O$ depends linearly on $\Delta\mu_O$, according to Eq. (2). Again the GGA interfacial energies are lower than the LDA values, but GGA and LDA trends and relative energies are similar. Note that as the oxygen partial pressure and $\Delta\mu_O$ increases, $Nb/(Al_2O_3)_O$ becomes more stable than $Nb/(Al_2O_3)_{Al}$. So the relative stabilities of the free $Al_2O_3(0001)$ surfaces are reversed by the addition of Nb to the surfaces. This is consistent with the data of Ref. 5, which reported oxygen termination for the $Nb(111)/\alpha\text{-}Al_2O_3(0001)$ interface. This is perhaps our most important result.

Let us examine this result more thoroughly. For larger $\Delta\mu_O$, we indicate in Fig. 3 that bulk oxides of Nb are formed. This is based[27] on the heat of formation of NbO being 4.21 eV, shown by a vertical dotted line at $\Delta\mu_O = -4.21$ in Fig. 3. We have not included oxides of Nb in our computations. Therefore our results apply strictly only to the range of oxygen partial pressures where the pressure is high enough that O can go to the interface to affect the $Al_2O_3(0001)$ termination, but not so high that substantial interfacial oxides of Nb are formed. Our results shown in Fig. 3 suggest that such a range exists. This is also consistent with the experimental results of Bruley *et al.*[5] on their $Nb(111)/\alpha\text{-}Al_2O_3(0001)$ interface produced by molecular beam epitaxy. See, in particular, their Fig. 7(b) and their corresponding discussion. Their data (see their Fig. 6), indicate oxides of Nb on the free Nb surface but not at the Nb/Al_2O_3 interface. As noted above, their data also indicate that the $Al_2O_3(0001)$ is oxygen-terminated at the interface. This is consistent with our results in Fig. 3. There we show that the $Nb/(Al_2O_3)_O$ interfacial energy moves below the $Nb/(Al_2O_3)_{Al}$ value at an oxygen chemical potential significantly below the onset of Nb oxide formation. Moreover, the oxygen-terminated interfacial energy continues to drop relative to the aluminum-terminated interfacial energy as the chemical potential moves into the region of Nb oxide formation. Again, this means that the oxygen-terminated interface is predicted to be stable under the experimental conditions of Ref. 5. These results are also consistent with the experimental results of Ref. 11, where it was reported that metal/alumina works of adhesion can depend on oxygen partial pressures.

TABLE IV. Energies in eV per Al atom, as described in the text.

E_S		E_I	E_V	
0.86	1.18[a]	5.17	2.73	3.03[b]

[a]Reference 30.
[b]Reference 31.

D. Al diffusion into Nb from Al_2O_3

Finally, let us examine further the $Nb/(Al_2O_3)$ interface. We attempt to provide information relative to the diffusion of Al from the Al_2O_3 into the Nb. This information is of interest because of the observation[28,29] of an Al concentration profile in the Nb associated with a diffusion bonded $Nb/(Al_2O_3)$. First, we compute some fundamental heats or energies we will need in this analysis. For all of these computations we used the computational methods described in Sec. II, within the (more accurate) GGA. First, we compute the heat of solution of Al (from bulk Al) in (bulk) Nb. Results can be found in Table IV. In the table, E_S is the heat of solution, where Al is taken to be substitutional in the Nb; E_I is the energy to form an interstitial Al atom (from bulk Al) in (bulk) Nb; and E_V is the vacancy formation energy for Nb. Our first-principles heat of solution E_S agrees reasonably well with the empirical value of Ref. 30. As expected, the formation of an interstitial Al in Nb is endothermic, and so the lower-energy configuration for Al in solution is substitutional. Our first-principles Nb vacancy formation energy also agrees well with the experimental value of Ref. 31.

TABLE V. Energies per Al atom in eV required to convert an $Nb/(Al_2O_3)_{Al}$ interface to an $Nb/(Al_2O_3)_O$ interface, with Al ending up in Nb interstitial sites (E_{1I}), substitutional sites (E_{1S}), or vacancy sites (E_{1V}).

E_{1I}	E_{1S}	E_{1V}
6.77	0.74	−1.99

Next, we compute one more term, which will be seen to be fundamental in determining energetics of interest for diffusion of Al in Nb. This is the energy E_D, where

$$E_D \equiv E_{\text{tot}}[\text{Nb}/(\text{Al}_2\text{O}_3)_O] - E_{\text{tot}}[\text{Nb}/(\text{Al}_2\text{O}_3)_{Al}] + \mu^B_{Al}. \quad (4)$$

Here μ^B_{Al} is the chemical potential of bulk aluminum, and so E_D is the energy to move Al atoms from the $Nb/(Al_2O_3)_{Al}$ interface to (a separate mass of) bulk Al. We find that $E_D = 1.60$ eV per Al atom. Now we are ready to compute quantities relevant to Al diffusion into Nb. We begin with the $Nb/(Al_2O_3)_{Al}$ interface, which we will call interface 1. Let us call E_{1I} the energy per Al atom associated with converting the $Nb/(Al_2O_3)_{Al}$ interface to an $Nb/(Al_2O_3)_O$ interface, with the Al atoms ending up at interstitial sites in the Nb. Then

$$E_{1I} = E_D + E_I. \quad (5)$$

We see from Table V that E_{1I} is 6.77 eV. That is, the state with the Al atoms at interstitial sites in the Nb and an $Nb/(Al_2O_3)_O$ interface is 6.77 eV per Al atom higher in energy than the state with the Al atoms forming the $Nb/(Al_2O_3)_{Al}$ interface. The obvious conclusion is that the $Nb/(Al_2O_3)_{Al}$ interface is stable relative to interstitial solution of the Al atoms in the Nb. The energy to move the Al atoms to the substitutional site is defined as E_{1S}, where

$$E_{1S} = E_D - E_S. \quad (6)$$

E_{1S} is determined to be 0.74 eV, substantially smaller than E_{1I}, but nevertheless the Nb substitutional site is higher in energy than the interfacial site. Finally, the energy to move the Al atoms to a vacancy site, E_{1V}, is

$$E_{1W} = E_D - E_V. \quad (7)$$

We find that this site is 1.99 eV lower in energy than the interfacial site. Note, however, that the number of vacancy sites is relatively low. Gaskell[32] estimates, e.g., that in bulk Al, even at a temperature as high as the melting temperature the fraction of vacant sites is only 9×10^{-4}.

At low temperatures, then, we would not expect significant diffusion of the Al atoms in the Nb. At higher temperatures, because of the *TS* term in Eq. (1), one might expect the Gibbs free energy of the dissolved Al state to be lowered relative to the state where there is no Al in the Nb if the entropy increase associated with diffusion is sufficiently high. While we were not able to find data for Al-Nb alloys, data[33] for the entropy increase associated with the formation of many Al alloys from elemental metals are in the range 0.6–1.5 cal/mol K at approximately 0.1 atomic fraction of Al. Of course our Al does not come from elemental Al, but rather from Al_2O_3. Nevertheless, if we take 1.0 cal/mol K = 0.43 eV/Al atom 10^3 K as an average entropy increase, then at 2,000 K the entropy increase would lower the relative Gibbs free energy of the dissolved Al state by 0.86 eV/Al atom. From Table V, we can see that this would make the Gibbs free energy of the substitutional state for the Al in Nb lower than the Al-free Nb state ($E_{1S}<0$). This suggests that diffusion bonding could lead to Al migrating from the Al_2O_3 to the Nb, consistent with reported experimental observations.[28,29]

Note, finally, that the above-noted analysis only examines in an average way the Gibbs energy associated with a part of the diffusional process. If Al atoms do manage to diffuse into the Nb from the Nb/Al_2O_3 interfacial region, presumably they are replaced in the interfacial region by Al atoms migrating to that region from the bulk of the Al_2O_3. Thus the Al_2O_3 termination in the Nb/Al_2O_3 interface is still determined by the considerations of Sec. III C above, even if there was diffusion of Al into the Nb.

IV. SUMMARY

We have carried out first-principles computations of atomic relaxations, electron-density contours, and energetics of Al_2O_3 surfaces and Nb/Al_2O_3 interfaces. These were done for both stoichiometric and nonstoichiometric surfaces and interfaces. We found substantial atomic relaxations for all these surfaces and interfaces, with interesting variations depending on Nb film thickness, Nb and Al size differences, and deviations from stoichiometry. Electron density contours show the transition between metallic and ionic bonding across the Nb/Al_2O_3 interface, as well as how the bonding varies between stoichiometric and nonstoichiometric surfaces and interfaces. The works of separation are independent of oxygen partial pressure, with the O-terminated value being over 3 times the Al-terminated value. All of the aforementioned results were obtained both in the local-density approximation (LDA), and in the presumably more accurate generalized-gradient approximation (GGA). While there are quantitative differences in the LDA and GGA results, predicted trends are similar and conclusions are essentially the same.

We showed that surface energies and interfacial energies depend on the oxygen chemical potential and corresponding oxygen partial pressures for nonstoichiometric interfaces. For the Al_2O_3 surface, the Al-terminated (stoichiometric) surface is stable, i.e., is lower in energy than the O-terminated surface, for the entire range of oxygen partial pressures. At sufficiently low oxygen chemical potentials and partial pressures, we also found that the stable Nb/Al_2O_3 interface contains Al-terminated Al_2O_3. However, as oxygen partial pressures and chemical potentials increase, the stable Nb/Al_2O_3 interface becomes O-terminated, consistent with recent experimental results.[5] That is, the formation of the interface with Nb can reverse the stability of the Al_2O_3 termination. While this is the first prediction of the stable interfacial structure for a metal/ceramic oxide interface, Saiz *et al.*[11] have reported a dependence of works of metal/Al_2O_3 adhesion on oxygen pressures, consistent with our results.

Finally, we determined some of the energetics associated with diffusion of the Al from the Al_2O_3 across the interface into the Nb. It seems unlikely that one would find substantial solution of the Al in the Nb, except at temperatures of order 10^3 K.

ACKNOWLEDGMENTS

The authors acknowledge, with thanks, numerous useful conversations with Professor Anthony Evans, including the formulation of plans for computations and the relation of our results to experimental results. We also would like to thank Dr. Roland Cannon for his guidance on oxygen partial pressures and stoichiometry. This work was supported in part by the NSF, under Grant No. NSF DMR9-98-05188.

[1] A. G. Evans, J. W. Hutchinson, and Y. Wei, Acta Mater. **47**, 4093 (1999).

[2] M. W. Finnis, J. Phys.: Condens. Matter **8**, 5811 (1996), and references cited therein.

[3] M. Wagner, T. Wagner, D. L. Carroll, J. Marien, D. A. Bonnell, and M. Rühle, Mater. Res. Bull. **1997**, 42.

[4] G. L. Zhao, J. R. Smith, J. Raynolds, and D. J. Srolovitz, Interface Sci. **3**, 289 (1996); see also T. Hong, J. R. Smith, and D. J. Srolovitz, Acta Metall. Mater. **43**, 2721 (1995); W. Zhang and J. R. Smith, Phys. Rev. Lett. **82**, 3105 (1999); J. R. Smith and W. Zhang, Acta Mater. (to be published).

[5] J. Bruley, R. Brydson, H. Mulleejans, J. Mayer, G. Gutekunst, W. Mader, D. Knauss, and M. Rühle, J. Mater. Res. **9**, 2574 (1994), and references cited therein; see also J. Mayer, C. P. Flynn, and M. Rühle, Ultramicroscopy **33**, 51 (1990).

[6] C. Kruse, M. W. Finnis, J. S. Lin, M. C. Payne, V. Milman, A. D. Vita, and M. J. Gillan, Philos. Mag. Lett. **73**, 377 (1996).

[7] I. G. Batirev, A. Alavi, and M. W. Finnis, Phys. Rev. Lett. **82**, 1510 (1999).

[8] G. Song, A. Remhof, K. Theis-brohl, and H. Zabel, Phys. Rev. Lett. **79**, 5062 (1997).

[9] M. Kohyama, S. Kose, M. Kinoshita, and R. Yamamoto, J. Phys. Chem. Solids **53**, 345 (1997).

[10] (a) R. Di Felice and J. E. Northrup, Phys. Rev. B **60**, R16 287 (1999); (b) see also X.-G. Wang, A. Chaka, and M. Scheffler, Phys. Rev. Lett. **84**, 3650 (2000) and X.-G. Wang, W. Weiss, Sh. K. Shaikhutdinov, R. Ritter, M. Petersen, F. Wagner, R. Schlogl, and M. Scheffler, Phys. Rev. Lett. **81**, 1038 (1998).

[11] E. Saiz, R. M. Cannon, and A. O. Tomsia, Acta Mater. **47**, 4209 (1999). See also D. Chatain, L. Coudurier, and N. Eustathopoulos, Rev. Phys. Appl. **23**, 1055 (1988).

[12] E. Wimmer, H. Krakauer, M. Weinert, and A. J. Freeman, Phys. Rev. B **24**, 864 (1981); P. Blaha, K. Schwarz, P. Dufek, and R. Agustyn, WIEN95 (Technical University of Vienna, Vienna, 1995); P. Blaha, K. Schwarz, P. Sorantin, and S. B. Trickey, Comput. Phys. Commun. **59**, 399 (1990).

[13] D. J. Singh, Phys. Rev. B **43**, 6388 (1991).

[14] W. Kohler, S. Wilke, M. Scheffler, R. Kouba, and C. Ambrosch-Draxl, Comput. Phys. Commun. **94**, 31 (1996).

[15] J. P. Perdew and Y. Wang, Phys. Rev. B **45**, 13 244 (1992).

[16] J. P. Perdew, K. Burke, and M. Ernzerhof, Phys. Rev. Lett. **77**, 3865 (1996).

[17] C. Verdozzi, D. R. Jennison, P. A. Schuyltz, and M. P. Sears, Phys. Rev. Lett. **82**, 799 (1999).

[18] R. W. G. Wyckoff, *Crystal Structures*, 2nd ed. (Interscience Publishers, New York, 1964), Vol. 2.

[19] J. Schnitker and D. J. Srolovitz, Modell. Simul. Mater. Sci. Eng. **6**, 153 (1998).

[20] C. Kittel, *Introduction to Solid State Physics*, 4th ed. (Wiley, New York, 1971).

[21] H. Wawra, Z. Metallkd. **66**, 395 (1975).

[22] I. Manassidis, A. D. Vita, and M. J. Gillan, Surf. Sci. **285**, L517 (1993).

[23] We got the same results for two different initial structures, both for Nb replacing the top Al layer. One corresponds to the case of the Nb atoms being at the bulk Al site location and another for the Nb atoms being at the surface site location of the relaxed $(Al_2O_3)_{Al}$ structure.

[24] The layer distance of the free-standing Nb(111) is 0.93 Å (LDA) and 0.95 Å (GGA). It decreases to 0.87 Å (LDA) and 0.90 Å (GGA) as Nb(111) is stretched to match $Al_2O_3(0001)$.

[25] A. Bogicevic and D. R. Jennison, Phys. Rev. Lett. **82**, 4050 (1999).

[26] *Physical Metallurgy*, edited by R. W. Cahn and P. Hassen (Elsevier Science BV, North-Holland, Amsterdam, 1996).

[27] *CRC Handbook of Chemistry and Physics*, 78th ed., edited by D. R. Lide (CRC Press, Boca Raton, FL, 1997).

[28] K. Burger, W. Mader, and M. Rühle, Ultramicroscopy **22**, 1 (1987).

[29] K. Burger and M. Rühle, Ultramicroscopy **29**, 88 (1989).

[30] F. R. De Boer, R. Boom, W. C. M. Mattens, A. R. Miedema, and A. K. Niessen, *Cohesion in Metals* (North-Holland, Amsterdam, 1988).

[31] H. J. Wollenberger, in *Physical Metallurgy*, 4th ed., edited by R. W. Cahn and P. Hassen (Elsevier Science BV, North-Holland, Amsterdam, 1996), Chap. 18.

[32] D. R. Gaskell, in *Physical Metallurgy* (Ref. 31), Chap. 5.

[33] R. Hultgren, P. D. Desai, D. T. Hawkins, M. Gleiser, and K. Kelley, *Selected Values of the Thermodynamical Properties of Binary Alloys* (ASM, Metals Park, OH, 1973).